

# SHEAR PERFORMANCE ESTIMATION OF WOODEN LATHS AND PLASTER WALLS THROUGH EXPERIMENTS AND NUMERICAL ANALYSIS

Naoyuki Matsumoto<sup>1</sup>, Katsuhiko Yamawaki<sup>2</sup>, Kaori Fujita<sup>3</sup>

**ABSTRACT:** Structural tests and analytical modelling were conducted to clarify the seismic performance of wooden laths and plaster walls, which are one of the representative types of modern Japanese wooden buildings. Wooden laths and plaster is a construction method where plaster is applied to substrates made with 50 mm wide and 10 mm thick boards. In this study, the plaster wall was fabricated with the four sides of the wall restrained by the frame (columns, a lintel, and a baseboard), and static lateral loading tests were conducted. The results indicated that the wall has two types of resistance mechanisms, one at the point of initial stiffness and the other at the point of reaching the maximum bearing capacity, due to the large influence of the wall restraint by the frame. Secondly, shear element tests of small walls and shear tests of plaster materials were conducted to simulate the two types of resistance mechanisms. Finally, two numerical analysis models were presented to estimate the initial stiffness and maximum bearing capacity in a full-scale test. The numerical analyses showed an initial stiffness of 80% and a maximum bearing capacity of 130%.

**KEYWORDS:** Wooden lath, Plaster, Lateral loading test, Element test, Shear performance, Analytical model

## 1 INTRODUCTION

### 1.1 BACKGROUND

Modern Japanese wooden buildings, from the Meiji Restoration to World War II, are built based on the mixed techniques of traditional and Western buildings, and many do not have reliable standards or data for structural evaluation. With the increase in the preservation and rehabilitation of modern wooden buildings, proper evaluations of their structural mechanisms are imminent. Few studies have focused on the structural systems of modern structural walls, and a variety of walls was found to have surplus capacity [1-3]. This study focuses on a wall with wooden laths as substrates and plaster as the finish. Although this type of wall is one of the most prevalent and existing experiments have reported the reinforcement effect of the plaster finish and its tough behavior, even after plaster failure, its structural mechanism has not yet been clarified. Therefore, establishing a numerical estimation method for evaluating the structural performance of wooden laths and plaster walls will lead to more flexible and appropriate seismic diagnoses and evaluations of modern wooden buildings.

### 1.2 PURPOSE AND METHODOLOGY

This study aims to experimentally elucidate the horizontal force resistance mechanisms of wooden laths and plaster walls and proposes a mechanical model to estimate the

initial stiffness and maximum load as the basic structural performance of the wall. Here, the composition pattern of laths was based on the Japanese style; that is, laths were nailed only between the columns on the small studs next to them (**Figure 1**).

First, we conducted full-scale lateral loading tests to understand the typical load deformation relationships and failure patterns and then proposed two phases of resistant systems. Subsequently, element tests on the shear performance of the plaster, lath-and-nails, and small laths-and-plaster walls were performed. Finally, in combination with the resulting data, an analytical model is proposed to assume the initial stiffness and maximum load.

## 2 WOODEN LATHS AND PLASTER

Wooden laths and plaster finishes quickly prevailed in Japan after the Meiji Restoration (1868), referring to the Western techniques and combining them with traditional plastering techniques. Thin wooden lath boards (approximately 50 mm wide and 10 mm thick) were used as substrates, and they were nailed to the columns. Hemp ropes were also nailed for fastening plaster and the laths, and plaster mixed with seaweed glue was applied in layers of approximately 20 mm. This method is commonly used for the walls of Western-style buildings as a substitute for mud walls and is sometimes applied to ceilings. **Figure 1** shows a schematic of wooden laths and plaster walls.

<sup>1</sup> Naoyuki Matsumoto, Department of Civil Engineering and Architecture, Faculty of Eng., Tohoku University, Japan, nmatsu@rel.archi.tohoku.ac.jp

<sup>2</sup> Katsuhiko Yamawaki, Yamawaki Katsuhiko Architectural Engineering Design, Inc., Japan, yamyam.e.design@gmail.com

<sup>3</sup> Kaori Fujita, Dep. of Arch., Faculty of Eng., The University of Tokyo, Japan, fujita@arch1.t.u-tokyo.ac.jp

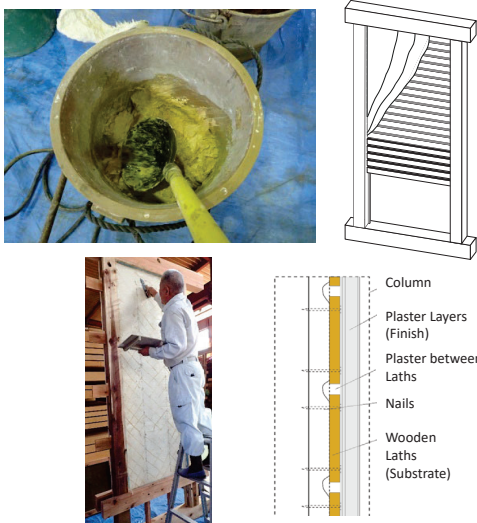


**Figure 1:** [clockwise from top left] Plaster material, Composition of the wooden laths and plaster wall, Section details of the wall, and Plastering process

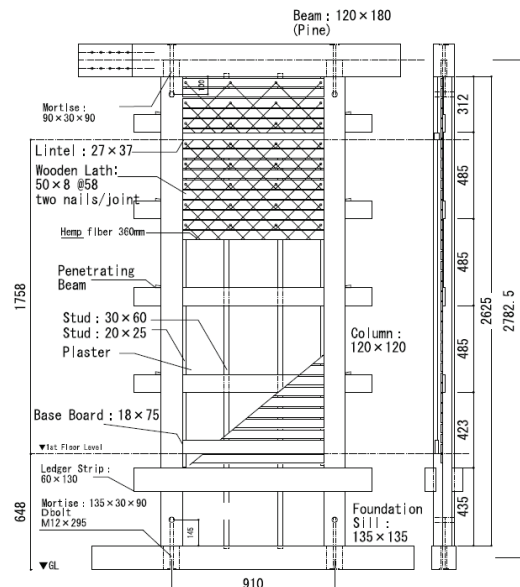


**Figure 2:** Dimensions of the specimen [lath and plaster + frame]

### 3 FULL-SCALE LATERAL LOADING TESTS

#### 3.1 SUMMARY OF LATERAL LOADING TESTS

Full-scale static loading tests were conducted to clarify the horizontal force resistance mechanisms of the wooden laths and plaster walls. The dimensions of the specimens were based on those of a cultural heritage house built in Tokyo in 1928. To understand clearly the differences in the structural performances and mechanisms, the same tests were conducted on a frame wall (only with penetrating beams) with the same dimensions.

#### 3.2 SPECIMENS

The specifications of the specimens are shown in **Figure 2**. The specimen was made with traditional unit wall dimensions of 910 mm × 2783 mm, referring to the walls of an important cultural property building located in Tokyo (constructed in 1928, modern Japanese-style architecture). The wall has four penetrating beams, two ledger strips at the bottom, and a void below the floor level. The wall was divided into upper and lower sections by a nailed lintel, and at the bottom of the plaster wall, a baseboard was inserted and nailed to the column.

The substrate of the wall was made of 50 mm wide and 8 mm thick wooden lath nailed to the pillar frames, and plaster was applied over the laths. The formulation of the plaster is listed in **Table 2**. Three types of plaster were used: undercoat, middle coat, and finish coat. The formulations conformed to the specifications of the buildings used as the reference. The materials used were slaked lime, sand, hemp fiber, seaweed glue, and water. The plaster material for each layer was prepared by first making a mixture of glue, slaked lime, and hemp fiber, called “*Tsuta-awase*,” and then mixing sand into the mixture as needed. The total plaster thickness was approximately 20 mm.

**Table 1:** Specifications of specimens [lath and plaster + frame]

Item	Unit	Dimension/Specification
Column	mm	120 × 120
Beam	mm	120 × 180
Foundation	mm	135 × 135
Stud	mm	30 × 60, 20 × 25
Species	—	Sugi (Japanese Cedar)
Wooden Lath	mm	50 × 8 × 530 @58
Species	—	Sugi (Japanese Cedar)
Nail	mm	N32 * 2 [30 mm apart] @255; shell diameter: 1.9

**Table 2:** Formulation of plaster

Number of layer	Types of layer	unit	Thickness of each layer	Note on formulation
1 <sup>st</sup> and 2 <sup>nd</sup> layer	Under coat	mm	t = 2+1	<i>Tsuta-awase</i> (Plaster with hemp) Slaked lime Water
3 <sup>rd</sup> layer	Flatten layer	mm	t = 1	Same as above
4 <sup>th</sup> , 5 <sup>th</sup> , and 6 <sup>th</sup> layer	Middle layer	mm	t = 4+3+3	Plaster : Sand = 1:2 (or more)
7 <sup>th</sup> layer	Finish coat	mm	t = 2	Plaster (shell ash) and algae glue

A static cyclic load ranging from 1/600 rad to 1/10 rad was applied, one cycle at each step. The test was terminated when the maximum load decreased to 80% or reached 1/10 rad.

### 3.3 RESULTS OF LATERAL LOADING TESTS

The maximum bearing capacity was 8.7 kN (at 1/60 rad). For the wooden lath and plaster wall, approximately 1.9 times higher than the 4.6 kN (at 1/15 rad) of the frame specimen. Elastic stiffness was 7.5 times greater for the wooden lath and plaster wall than for the frame specimen. The deformation angle at the maximum load capacity was +1/60 rad to -1/75 rad for the wooden lath and plaster wall, whereas the load did not decrease for the frame specimen.

Although the frame wall exhibited some damage to the penetrating beams and ledger strips by embedding, the load increased toward the end of the experiment, at 1/10 rad. In contrast, the wooden lath and plaster wall initially showed a stable high stiffness value; however, after exceeding the maximum load capacity, the load decreased to approximately 60% of the maximum load capacity, indicating a brittle behavior. Subsequently, the load gradually increased and was 1.5 times greater than that of the frame specimen, suggesting that the nails and residual plaster were functional up to large deformations.

Based on the observation of the failure conditions, the resistance mechanism of the wooden plaster and lath wall to horizontal forces can be divided into two phases.

The restraint condition of the plaster layer changes as the deformation progresses and the two lateral members (lintel and baseboard) that support the layers gradually break at their connections with the columns. When the two lateral members and joints are sound, as the initial stiffness is maintained, the shear and compression performances of the plaster are dominant, because the four-round members restrain the plaster layer. However, at approximately the maximum load after the loss of the baseboard restraint, the plaster layer was mainly restrained to only two columns, and the plaster layer began rotating. Then, the lateral resistance is dominated by the rotation-shear force between the plaster layer and the plaster filling the gap between the laths. Based on these two phases of resistance mechanisms, we propose an “initial stiffness estimation model” and a “maximum strength estimation model.”

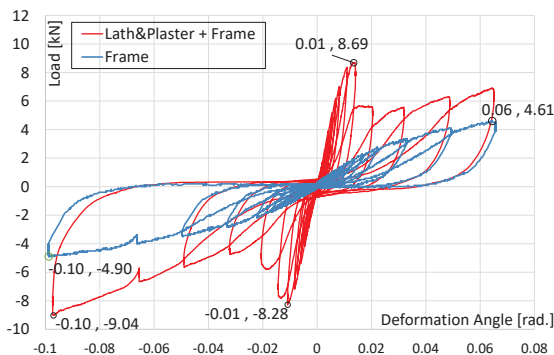


Figure 3: Comparison of test results for wooden laths and plaster wall and frame wall (columns and beams)

Table 3: Characteristic value of full-scale wall test

Characteristic value	Maximum Deformation Yield Strength		Yield Deformation Strength		Ultimate Deformation Strength		Ultimate Deformation Stiffness	
	$P_{max}$	$\delta_{pmax}$	$P_y$	$\delta_y$	$P_u$	$\delta_u$	$K$	
	unit	kN	rad.	kN	rad.	kN	rad.	kN/rad.
Frame	Push	4.61	0.065	2.71	0.024	4.13	0.067	114
	Pull	4.02	0.066	2.37	0.027	3.51	0.067	89
	Ave.	4.31	0.065	2.54	0.025	3.82	0.067	102
Lath and Plaster + Frame	Push	8.69	0.016	5.69	0.007	6.10	0.033	768
	Pull	8.28	0.014	5.27	0.007	5.72	0.034	784
	Ave.	8.49	0.015	5.48	0.007	5.91	0.033	776

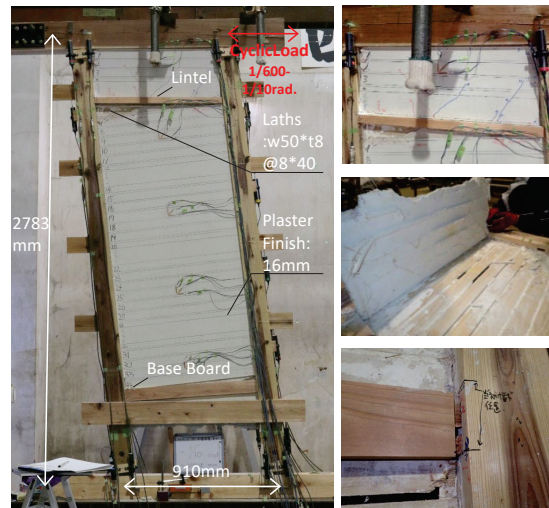


Figure 4: (Left) Ultimate condition of wooden laths and plaster wall (@-1/10 rad). (Right): Major fracture patterns of wooden laths and plaster (shear and compressive failures of the plaster layer, shear failure of the plaster filled within wooden laths' gaps, and fracture at the edge of base board)

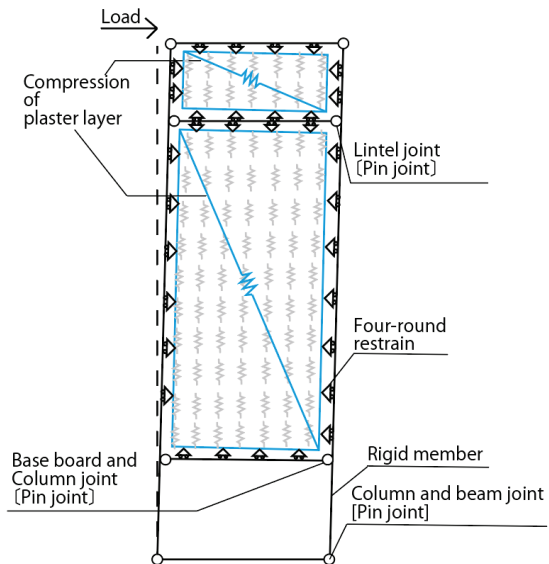
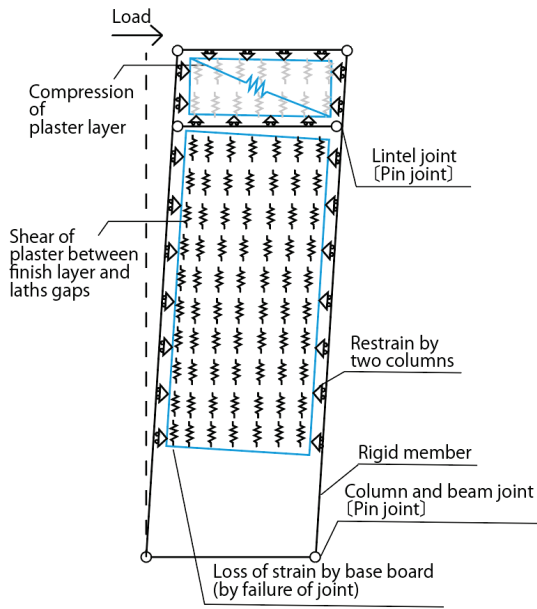


Figure 5: Lateral resistant mechanism of laths and plaster wall: initial stiffness phase



**Figure 6:** Lateral resistant mechanism of laths and plaster wall: maximum load phase

#### 4 ELEMENT TESTS ON WOODEN LATHS AND PLASTER

Two types of element tests were conducted to determine the properties required to fulfil the analytical model: (1) shear tests on 580 mm square small laths and plaster walls, and (2) shear tests on the plaster material

##### 4.1 SHEAR TESTS ON 580 MM SQUARE SMALL LATH AND PLASTER WALL

From the observations of the full-scale tests, it was estimated that the shear resistance of the wooden lath and plaster wall, when fully restrained on all four sides, is mainly due to the shear resistance of the nails, compressive effect of the wooden lath and plaster wall, and shear resistance of the plaster key. To verify these effects, elemental specimens of 580 mm square lath and plaster walls were prepared, and shear element experiments were conducted with and without plaster as parameters. The specimens are shown in **Figure 8**. The specifications of the wooden lath and plaster element wall were identical to those of the full-scale specimen.

##### WL series: Specimens without plaster finish

As the specimen deformed in shear, shear deformation occurred at the joints of each wooden lath to the supporting wood at the edge by the nails and studs. The distance between the edge of the wooden lath and the wood frame was approximately 1 to 1.5 mm, and the contact between the wood frame and the edge of the wooden lath was observed to be approximately 1/15 rad. Subsequently, the nails of the wood-frame support were pulled out and embedded in the wood frame. Although the load did not decrease, cracks and fractures were observed at the edges of the wooden lath. The maximum loads of three specimens were 1.4 kN (0.11 rad.), 1.4 kN (0.12 rad.), and 0.6 kN (0.1 rad.).

##### WL+P series: Specimens with plaster finish

In the test of WL+P1, the plaster layer gradually began to swell and went up on the wooden frame before it reached the maximum load. Eventually, the shear failure of the plaster at the gap between the wooden laths and the crushing of the plaster layer at the top and bottom edges occurred. However, shear cracks were not observed. However, in the case of WL+P2, although slip was observed at the beginning, the plaster layer did not protrude, but resisted within the wooden frame surface, and the load decreased after the deformation angle of 0.03 rad. Cracks were observed between the top and bottom at a deformation angle of approximately 1/22 rad. In both specimens, the behavior was similar; compression between the top and bottom edges became remarkable, as the plaster layer did not follow the shear state in the large deformation. The maximum load was 10.7 kN (0.03 rad) for WL+P1 and 9.7 kN (0.036 rad) for WL+P 2.

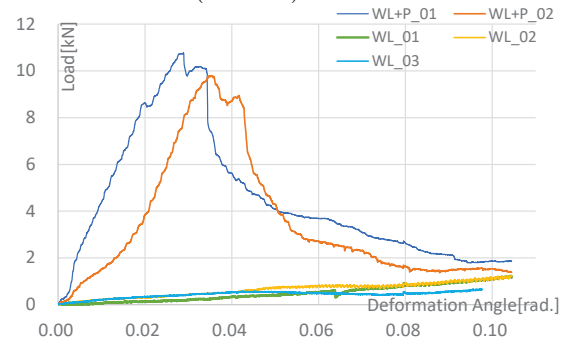


**Figure 7:** Results of the Test: WL+P (wooden laths and plaster) and WL (wooden laths)

**Table 4:** Characteristic value of small wall shear tests

Characteristic Value	Max Load	Angle at Max Load	Elastic Shear Stiffness*
	kN	rad.	kN/mm <sup>2</sup> ·rad.
Wooden Lath (WL)	1	1.40	0.1 **0.002
	2	1.40	0.1 **0.002
	3	0.60	0.1 **0.0005
	ave.	1.13	0.1 —
Wooden Lath + Plaster (WL+P)	1	10.7	0.03 0.06
	2	9.7	0.036 0.03—0.04
	ave.	10.2	0.033 —

\* 2 kN to 8 kN are regarded as the elastic area

\*\*Shear area of WL series are assumed to be same as WL+P

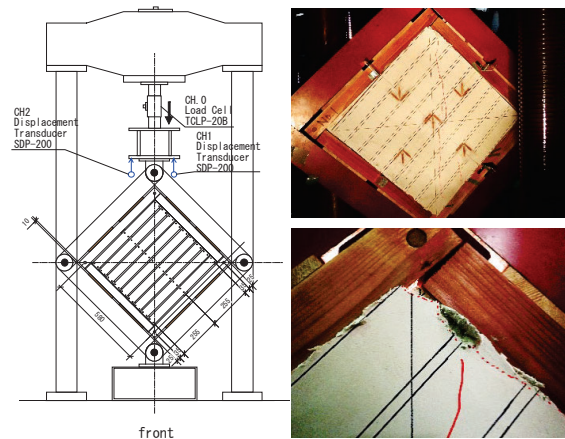


**Figure 8:** Setting of shear tests(left), Final condition of shear tests of small wall: (cracks on plaster(up), Crushed plaster edge(down))

## 4.2 SHEAR TESTS ON PLASTER MATERIAL

Based on the observation of the full-scale test, it was assumed that the plaster key between the wooden laths would reach the maximum load by shear resistance as a resistance mechanism after the failure of the baseboard. Therefore, material shear tests were conducted on the undercoat plaster to determine its shear stiffness and strength.

### Maximum Shear Stress and Failure Process

The experimental results are listed in **Table 5**, and the load-deformation relationships are shown in **Figure 11**. The shear stress,  $\tau$ , was calculated by dividing the load by the shear area ( $B * H$ ), and was generally 0.7–0.8 N/mm<sup>2</sup> for the other specimens, although it was about 1.5 times higher for PS6 and PS7. The overall average is approximately 0.89 N/mm<sup>2</sup>. The displacement at the maximum load varied slightly from 0.64 to 1.6 mm, but the failure process was similar. Even after the shear face failed, the load gradually decreased as the plaster fragments became entangled with the fibers of the shear plane (**Figure 10**). However, edge collapse was observed under the applied force.

### Assumption of shear strain angle and elastic stiffness: Comparison with wood plaster

Because it was difficult to measure the shear strain directly, the following assumptions were made: The steel base that holds the specimen down has a 2 mm clearance from the shear plane of the plaster to remove the effect of compression at the corner. Considering the failure situation and assuming that the shear deformation in this area is significant and that the stress distribution is uniform, the shear strain  $\gamma$  is expressed as  $d/2$ , where  $d$  is the vertical displacement (**Figure 12**). The shear elastic stiffness calculated with shear strain  $\gamma$  was approximately 3 N/mm<sup>2</sup>.

In contrast, shear deformation was estimated to occur close to the surface of the actual plaster wall (**Figure 12**). In addition, because the undercoat plaster and plaster key are integrated, it is assumed that this area (thickness  $L$ ) is subjected to shear deformation if the plaster is sufficiently fixed in the gaps of the wooden laths. In this case, it was estimated that the size of the gap between laths affects the maximum shear force and has little effect on the failure displacement.

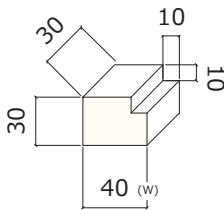


**Figure 9:** Dimensions of specimens (left)  
**Figure 10:** Final condition of shear tests (right)



**Table 5:** Result of shear tests

	$P_{max}$	$\tau_{max}$	Disp. @ $P_{max}$	Shear Strain @ $P_{max}$	Shear Stiffness*
unit	N	N/mm <sup>2</sup>	mm	-	N/mm <sup>2</sup>
PS1	421	0.70	0.64	0.32	3.43
PS2	486	0.81	1.00	0.50	2.39
PS3	435	0.83	0.88	0.44	5.19
PS4	460	0.77	1.60	0.80	1.13
PS5	454	0.78	1.54	0.77	2.22
PS6	669	1.17	0.80	0.40	4.98
PS7	698	1.15	1.52	0.76	1.70
Average	518	0.89	1.14	0.57	3.01

\*Secant stiffness from 10% to 50% of  $P_{max}$

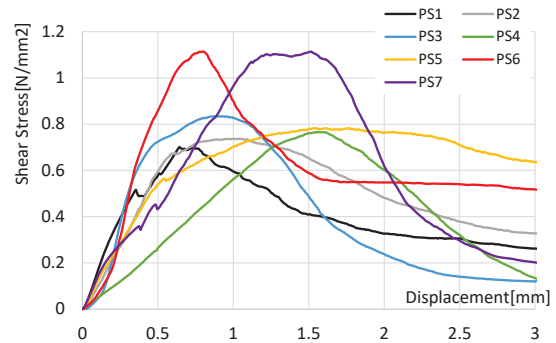


**Figure 11:** Shear stress–displacement curves

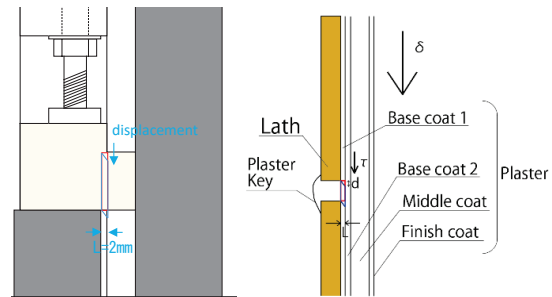


**Figure 12:** Settings of shear tests(left) and Hypothesis of Shear Strain in the wall (right)

## 5 ANALYSIS OF THE INITIAL STIFFNESS AND MAXIMUM LOAD

Two mechanical models were constructed based on previous tests to analyze the initial stiffness and maximum load. In the initial stiffness estimation model, in which the shear resistance of the wooden lath and plaster (both above and below the lintel) were considered, the shear stiffness was estimated to be approximately 80% accurate. In the model for estimating the maximum load, in which the shear resistance between the finish layer and the gaps of laths was dominant, particularly below the lintel, the maximum load was estimated to be approximately 1.3 times that of the tests. (**Figure 15**)

The horizontal shear stiffness and capacity of the wooden lath and plaster wall were calculated based on the results of the element tests described in Section 4. The calculation was performed on the portion of the wall that did not include the shear resistance of the frame wall (only the effects of the wooden lath and plaster were calculated).

In Section 3, the resistance mechanism of the Japanese-style (rounded by frames) plaster wall is divided into two phases, before and after the baseboard is damaged. The initial stiffness is assumed to be exerted mainly by the shear mechanism of the wall before the baseboard is damaged. The maximum bearing capacity was assumed to be reached through the process of shear failure of the plaster in the gap of the lath after the baseboard was damaged.

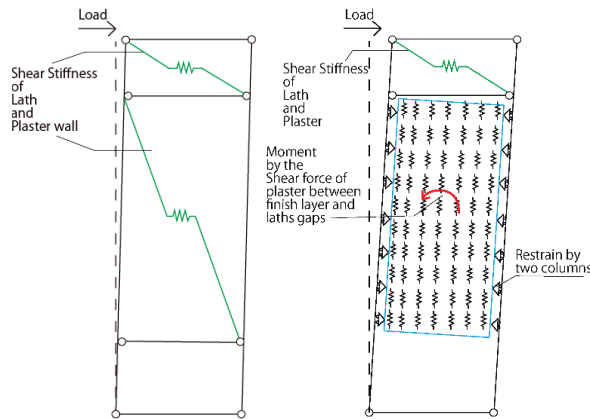


**Figure 13:** Analytical model of lath and plaster wall: Initial stiffness phase (left), Maximum strength phase (right)

### 1) Sound baseboard condition (initial stiffness model)

In the initial state of resistance, the lath and plaster walls were considered to act as shear-resisting elements. As shown in **Figure 13**, the stiffness and strength of the small-wall experiments were used to evaluate the initial stiffness.

The wall parameters applied to the initial stiffness model are as follows

$$\tau_{max} = P_{max} / \sqrt{2} / L / t = 0.067 \text{ [kN/cm}^2\text{]}$$

The initial stiffness of the hanging wall section is 88 [kN/cm<sup>2</sup>] and that of the section from the lintel to the baseboard is 422 [kN/cm<sup>2</sup>], totaling about 509 kN/cm<sup>2</sup>, which is about 80% of the experimental elastic stiffness (**figure 15**).

### 2) After baseboard failure (maximum bearing capacity)

From the observations of the full-scale test, it was estimated that when the base boards were damaged, the vertical restraining effect of the plaster layer was lost. In such a case, as explained in the previous section, it was assumed that the small area between the plaster and wooden lath substrates would resist shear deformation.

In the maximum bearing capacity model, the maximum bearing capacity is calculated based on the shear stiffness of the plaster. It is assumed that the upper and lower restraints are burned out and that only the left and right columns are restrained. The wooden frame was assumed to deform horizontally, whereas the plaster plate on the laths was assumed to deform rotationally while being restrained on the left and right sides. The load-deformation relationship for each angle of deformation

was calculated from the balance between the total moment resistance owing to the shear force from the plaster key between the wooden laths and the horizontal force acting on the top. (**Figure 14**) The maximum bearing capacity was 9.1 kN, approximately 1.3 times of the experimental value, as shown in **Figure 15**.

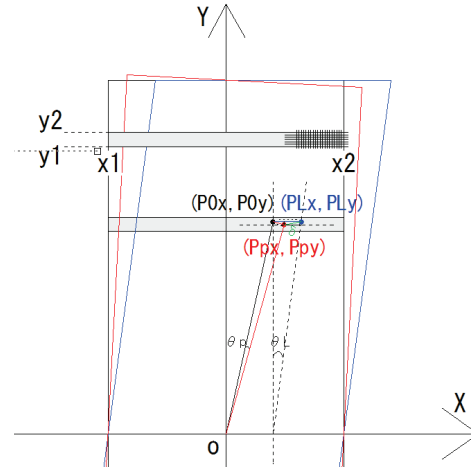


**Figure 14:** Diagram of shear displacement of plaster key (plaster between the gaps of laths) from wooden lath

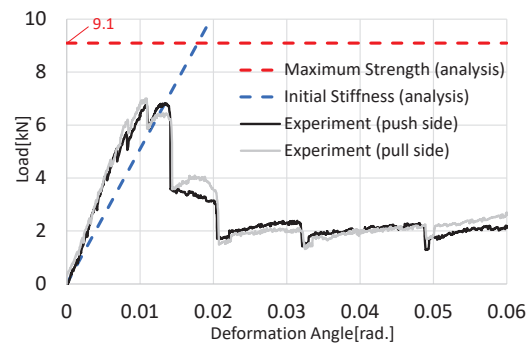


**Figure 15:** Shear stress–displacement curves showing the shear test evaluations and shear strain hypothesis

## 6 CONCLUSIONS

Lateral loading tests were conducted on laths and plaster walls to clarify their shear performances and failure mechanisms. The results indicate that the restraint conditions of the plaster layer (columns, lintel, and baseboard) significantly affected the resistance mechanism. Through element tests and analysis, we could accurately predict the initial stiffness (80% of the experiment) and maximum load (130% of the experiment). To clarify the proposed system further, the interactive behavior and stress distribution between the plaster and the laths must be investigated in detail.

## ACKNOWLEDGEMENT

The authors would like to thank Japan Cultural Heritage Consultancy, Iwase Kenchiku and Osaki Sakan for technical assistance with the production of specimens and conducting the experiments. This work was supported by JSPS KAKENHI 21K14287, Matsui Kakuhei Memorial Foundation and Obayashi Foundation.

## REFERENCES

- [1] Tanabe H., Goto K., Kikuta M.: Tests on Timber Frames with Wall (European System) under Alternate Horizontal Load (Study on Earthquake Resistant Timber Construction. Part 7)., *Journal of Architectural Institute of Japan*, 13:210-219, 1939.
- [2] Katayama T., Tomitaka R., Sawada K., Hirai T.: Structural Evaluation of Bearing Wall in Kita Ichijo Catholic Church, In: *Proceedings of the Annual Conference of Hokkaido branch of the Japan Wood Research Society*, 14-17, 2012.
- [3] Takino A., Shimokawa C., Ishiyama H., Nakano R.: Experimental Study on Lateral Performance of Shear Wall of Modern Timber Architecture Combined with Brace and Plaster using Wood Lath. *Journal of Structural and Construction Engineering*, 83(752):1477-1485,2018.